Z. Phys. D – Atoms, Molecules and Clusters 16, 97–106 (1990)

Atoms, Molecules and Clusters
Zeitschrift für Physik D

$KL_{2,3}$ ionization in neon by electron impact in the range 1.5–50 keV: cross sections and alignment

A. Albiez, M. Thoma, W. Weber, and W. Mehlhorn

Fakultät für Physik, Universität Freiburg, Hermann-Herder-Strasse 3, D-7800 Freiburg, Federal Republic of Germany

Received 5 February 1990

We have measured the ratio of cross sections $\sigma(KL_{2,3})/\sigma(K)$ for neon for electron impact in the energy range of $E_0 = 1.5 \ldots 50$ keV via the intensity of $KL_{2,3} - LLL_{2,3}$ Auger satellite lines relative to the intensity of $KL_1L_{2,3}(^3P)$ diagram line. The experimental ratio decreases over the full range of energy E_0 which is contrary to an earlier result by Carlson et al. We have also measured the alignment of $KL_{2,3}$ ^1P and ^3P states via the angular distribution of Auger satellite intensity for the energy range $E_0 = 1.5 \ldots 4$ keV, within experimental error we have found a zero alignment. The total K Auger spectrum, measured for $E_0 = 40$ keV and at the magic angle of emission $\vartheta = 54.7^0$, has been decomposed into its components by using appropriate line shapes distorted by postcollision interaction. Finally, we discussed whether the lines observed at the high-energy side of $KL_{2,3} - LLL_{2,3}$Auger satellite lines can be interpreted as structures caused by an angular momentum exchange in the postcollision interaction predicted by Niehaus and Zwakhals.

PACS: 34.80.D; 32.80.H

1. Introduction

The mechanism for L shell ionization simultaneously with the K shell ionization for electron impact is believed to be the electron shake-off [1–4]. If the velocity of both the impact electron and the ejected K shell electron is large enough compared to the orbital velocity of the outer L shell electron then the sudden approximation is valid [1–4] and the probability for shake-off of the L shell electron should become independent of the energy of the impact electron. Experimentally, the ratio of ionization cross sections $\sigma(KL_{2,3})/\sigma(K)$ of neon for electron impact, measured via the intensities of satellite and diagram Auger lines, has been found to be independent of the energy E_0 of electrons if $E_0 > 4.5\,E(KL_{2,3})$ ($E_0 > 4$ keV), where $E(KL_{2,3})$ is the energy to ionize in the K and $L_{2,3}$ shell [1]. The energy range E_0 investigated was $E_0/E(KL_{2,3}) = 1 \ldots 8$ which corresponds to $E_0 = 0.9 \ldots 7.5$ keV [1]. From this investigation it was concluded that for electron impact ionization of the K shell the sudden approximation is apparently reached for $E_0 > 4.5\,E(KL)$.

On the other hand, in a recent investigation of the ratio $\sigma(KL)/\sigma(K)$ for electron impact in low Z elements (solid targets with $Z = 9 \ldots 29$) via the intensities of X-ray satellite and diagram lines in the energy range of incident electrons $E_0 = 10 \ldots 200$ keV it was found [5], that $\sigma(KL)/\sigma(K)$ decreases in the full range of primary energy up to 200 keV. This contradictory result to the earlier finding of Carlson et al. [1] was explained by Löw et al. [5] by means of the original theory for multiple ionization by electron impact given by Åberg [6, 7]. From the energy dependence of cross sections [6], Löw et al. [5] derived an approximate expression for the ratio of cross sections

$$\sigma(KL_{2,3})/\sigma(K) = a + b(\ln E)^{-1}, \tag{1}$$

where a and b are energy independent terms and $E = E_0/E(KL)$. Neglecting electron correlation between the ejected K shell electron and the remaining bound electrons, the term a can be expressed by overlap matrix elements occuring in the shake model with sudden approximation [5, 6], which e.g. for Ne is given by [8]

$$a \cong \frac{\int_0^\infty \mathrm{d}\varepsilon |\langle 1s'\,2s'^2\,2p'^5(^{1,3}P)\varepsilon p'\,^2S|1s\,2s^2\,2p^6\,^2S\rangle|^2}{|\langle 1s'\,2s'^2\,2p'^6\,^2S|1s\,2s^2\,2p^6\,^2S\rangle|^2} = P(KL_{2,3})/P(K). \tag{2}$$

Here the unprimed and primed orbitals refer to the relaxed wavefunctions in the neutral ground state and in the K shell ionized state, respectively. The $P(K)$ and $P(KL_{2,3})$ are the probabilities in sudden approximation that in the event of sudden K shell ionization either all other electrons remain in their orbitals or one $2p$ electron is excited to the εp continuum state.

From (1) one would expect that only for an infinitely large impact energy E the ratio $\sigma(KL_{2,3})/\sigma(K)$ becomes constant. In fact, the value for b in (1) for neon can be obtained by interpolation from the results of Löw et al. (Fig. 3 of [5]) and is $b=0.10(5)$. Thus, in the range of energy $E=4.5 \ldots 8$, where in the experiment by Carlson et al. [1] an energy independent ratio $\sigma(KL_{2,3})/\sigma(K)$ was found, the energy dependent term of (1) changes from about 21.5% to 17% of the total value of $\sigma(KL_{2,3})/\sigma(K)$ (for the term a the value 0.224 [5] was taken). This decrease of about 4.5% of cross section ratio within the energy range $E=4.5 \ldots 8$ is within experimental errors still compatible with the cross section ratios measured by Carlson et al. [1], i.e., their experimental results could have been interpreted also by an energy dependent ratio of cross sections.

On the other hand, both experiments suffer from the fact that the intensities of Auger electrons [1] and X-rays [5] were measured at an angle $\vartheta=90°$ relative to the ionizing electron beam, and the observed energy independence [1] or energy dependence [5] of cross section ratio could originate from an energy dependent alignment of the $KL_{2,3}$ states. Although a pure shake-off process following a K shell ionization cannot create a non-zero alignment of the double vacancy state, e.g. $KL_{2,3}\,{}^1P, {}^3P$ in the present case, there might be small contributions to the $KL_{2,3}$ ionization from double collisions of the primary electron or a direct collision of the ejected K shell electron which very well may lead to an energy dependent alignment. In fact, the observed 20% increase of cross section ratio $\sigma(KL_{2,3})/\sigma(K)$ for neon for $E<4.0$ was partly interpreted by double collisions [1]. It is also well known, that for proton impact ionization in $KL_{2,3}$ shells of low elements considerable alignment occurs [9–11] which is fully explained by double collisions of the heavy projectile [12, 13].

In order to clarify this situation for the $KL_{2,3}$ ionization of neon by electron impact we have performed the following investigations:

1) We have measured the ratio $\sigma(KL_{2,3})/\sigma(K)$ of neon as function of impact energy in the energy range $E_0=1.5 \ldots 50$ keV ($E=E_0/E(KL_{2,3})=1.6 \ldots 54.3$) via the intensities of the $KL_{2,3}-LLL_{2,3}$ Auger satellite lines D11, D13, D14 and D15 [14] relative to the $KL_1L_{2,3}({}^3P)$ diagram line A3; the Auger electrons were measured at the magic angle $\vartheta=54.7^0$ relative to the primary electron beam.

2) In the energy range $E_0=1.5 \ldots 4.0$ keV of electron impact we have measured the alignment of double vacancy states $KL_{2,3}\,{}^1P$ and ${}^3P$ of neon via the angular distribution of Auger satellite electrons.

3) At an impact energy of $E_0=40$ keV the full K-Auger spectrum was measured and the relative intensities of all lines were determined.

2. Angular distribution formulas

Impact ionization of the K shell of an atom with initially closed shells leads to a zero alignment and the subsequent Auger transitions have an isotropic angular distribution [15]. As it was already pointed out in the introduction, the mechanism of shake-off following an ionization event with zero alignment cannot lead to an alignment $\neq 0$. On the other hand, we will assume that at least part of the double ionization $KL_{2,3}$ is due to multiple collisions which would lead to an alignment $\mathscr{A}_{20}$ of double vacancy states $1s2s^2 3p^5\,{}^1P$ and ${}^3P$. In the subsequent Auger transitions

$$\mathrm{Ne}^{2+}(1s2s^2 2p^5\,{}^1P, {}^3P) \rightarrow \mathrm{Ne}^{3+}(J_f S_f L_f) + e^-$$

the Auger electrons are ejected with an anisotropic angular distribution [16] (in the following we use the notation of Berezhko et al. [17])

$$I(\vartheta)=\frac{I_0}{4\pi}\{1+\mathscr{A}_{20}\alpha_2 P_2(\cos\vartheta)\}. \tag{3}$$

Here, I_0 is the total intensity of the Auger line, $\mathscr{A}_{20}$ is the parameter characterizing the alignment of the initial double vacancy state, α_2 is the decay parameter depending on the angular momenta of the initial and final Auger state and, in general, on the Auger decay amplitudes. Finally, P_2 is the second Legendre polynomial and ϑ is the angle of ejection relative to the beam of incident electrons.

In the following we consider the angular distributions of those satellite Auger transitions which have been presently investigated (the notation as D lines is taken from [14]):

$$\begin{aligned}
&1.\ 1s2s^2 2p^5({}^3P) \rightarrow 1s^2 2s^2 2p^3({}^2P),\ \text{line D11},\\
&2. \qquad\qquad\quad \rightarrow 1s^2 2s^2 2p^3({}^2D),\ \text{line D13},\\
&3.\ 1s2s^2 2p^5({}^1P) \rightarrow 1s^2 2s^2 2p^3({}^2P),\ \text{line D14},\\
&4. \qquad\qquad\quad \rightarrow 1s^2 2s^2 2p^3({}^2D),\ \text{line D15}.
\end{aligned} \tag{4}$$

Since we assume that the ionization is only due to the Coulomb interaction, it follows that the alignment parameter $\mathscr{A}_{20}$ is independent of the spin of the doubly ionized state, i.e., $\mathscr{A}_{20}$ is equal for the ${}^1P$ and ${}^3P$ initial states. The alignment parameter $\mathscr{A}_{20}$ can be expressed in terms of substate cross sections $\sigma(M_L)$ of the initial $({}^{1,3}P, M_L)$ states

$$\mathscr{A}_{20}({}^{1,3}P)=\sqrt{2}\,\frac{\sigma(M_L=1)-\sigma(M_L=0)}{2\cdot\sigma(M_L=1)+\sigma(M_L=0)}. \tag{5}$$

Furthermore, the fine structure splitting of the initial and final Auger states (4) are small compared to the line width Γ of Auger lines. In this case the parameter α_2 is determined only by the orbital angular momenta of the states and of the electrons involved in the Auger transition [18, 19]:

$$\alpha_2=\frac{\hat{L}_i \sum\limits_{l\leqq l'} (-1)^{L_i+L_f}\hat{l}\hat{l}'(l0\,l'0|k0)\begin{Bmatrix} L_i & L_i & k\\ l' & l & L_f\end{Bmatrix}(2-\delta_{ll'})\cdot \mathrm{Re}\,M_l M_{l'}}{\sum\limits_l |M_l|^2}. \tag{6}$$

Here L_i and L_f are the orbital angular momenta of the initial and final Auger states, l and l' are the angular

momenta of ejected partial Auger waves, M_l and $M_{l'}$ are the corresponding Auger transition amplitudes, $\delta_{ll'}$ is the Kronecker symbol, $\hat{l}=\sqrt{2l+1}$, $(....|..)$ is the Clebsch-Gordan coefficient and $\{\ \}$ is the $6j$-coefficient.

In the case of transitions 2 and 4 (lines D13 and D15) of (4) only a d Auger wave is ejected; then the parameter α_2 does not depend on the transition amplitude and can simply be evaluated from (6) to yield

$$\alpha_2(\mathrm{D13, D15})=1/\sqrt{2}. \tag{7}$$

This result together with $\mathcal{A}_{20}$ of (7) had been obtained already earlier [20]. For the evaluation of the parameter α_2 for the transitions 1 and 3 (lines D11 and D14) of (4) one needs also the transition amplitudes of s and d partial Auger waves. From the results given by Kabachnik et al. [18], the value for α_2 can be extracted and is

$$\alpha_2(\mathrm{D11, D14})=-0.59. \tag{8}$$

If the decay of the $KL_{2,3}$ vacancy states is observed via the X-radiation and the detection is polarisation dependent (as in [5] with crystal reflection) then the intensity $J(\vartheta, \psi)$ measured in direction ϑ relative to the primary electron beam is given by [21]

$$J(\vartheta, \psi)\sim\frac{I_0}{4\pi}\{1+\mathcal{A}_{20}\alpha_2^{\gamma}[P_2(\cos\vartheta)-\tfrac{3}{2}Q\sin^2\vartheta\cos 2\psi]\}. \tag{9}$$

Here a_2^{γ} is the decay parameter for the X-ray transition, Q is the polarisation sensitivity of the detector and the angle ψ is given by the orientation of the polariser axis of the detector relative to the plane determined by the directions of the beam and the observation.

3. Apparatus and experimental procedure

The apparatus, consisting of a target chamber, a 150° spherical sector electron spectrometer (with mean radius $r_0=238.5$ mm) and a channeltron detector, and which was described already earlier [22, 23], was extended in order to install a rotatable electron gun (energy range 0.5–4 keV) in the target chamber for the measurements of angular distributions of Auger electrons and to connect a high-energy electron gun (10–50 keV) to the target chamber with beam direction at the magic angle $\vartheta=54.7°$ relative to the detection direction of Auger electrons (see Fig. 1). The electron beam of either of the electron guns passed through the target cell which, in order to increase the target pressure, was part of a differential pumping system (P2 in Fig. 1). The gas inlet to the cell was via a thin metal tube, yet we assume that inside the cell the target density distribution was homogeneous. The target pressure inside the cell was about $4\cdot10^{-3}$ mbar with a pressure in the target chamber of about $2\cdot10^{-5}$ mbar, the pressure in the spectrometer chamber was always below $3\cdot10^{-6}$ mbar. The high-energy electron gun had its own pumping system (P4 in

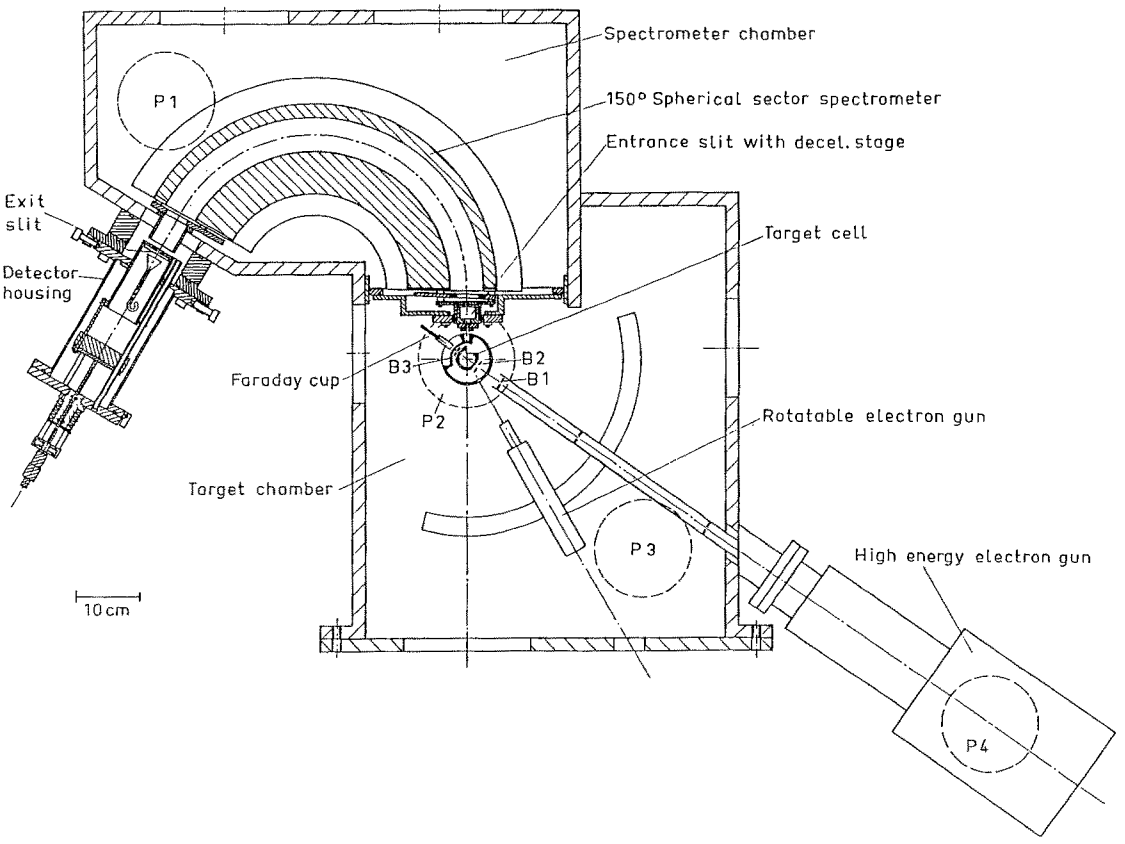

Fig. 1. Cross section of apparatus. P1 to P4 are pumps, B1 to B3 are circular slits for collimating the electron beam

Fig. 1) which provided a vacuum better than $3 \cdot 10^{-6}$ mbar.

The primary electron beams were well collimated by a series of circular slits, the slits before and behind the target cell (B_1, B_2 and B_3 in Fig. 1) were isolated in order to get a measure of the quality of collimation via the current on these slits. The slit currents on B_2 and B_3 were always $<10^{-3}$ of the cup current on the Faraday cup. For each of the two beam directions of $\vartheta = 54.7°$ and 90°, which were actually used in the experiment, individual target cells were constructed and interchanged accordingly.

The energy resolution of the spectrometer was $\Delta E/E = 5 \cdot 10^{-4}$, in a few cases the resolution was improved to about $3 \cdot 10^{-4}$ by decelerating the electrons before they entered the spectrometer. The earth's magnetic field was shielded by a single layer of μ-metal inside the apparatus which had been extended to include also the high-energy electron gun, and in addition it was compensated by the field of two pairs of Helmholtz coils to less than 1% of its field strength. For a further description of the experimental procedure see Weber et al. [23].

4. Experimental results and discussion

4.1. Ratio of cross sections $\sigma(KL_{2,3})/\sigma(K)$ as function of energy of primary electrons

Double ionization in $1s2p$ leads to ^1P and ^3P initial states and to a total of 13 satellite lines $KL_{2,3}-LLL_{2,3}$ [24, 14]. In order to determine the cross section ratio $\sigma(KL_{2,3})/\sigma(K)$ as function of the energy E_0 of primary electrons we measured the intensities of the strongest satellite lines, the lines D11 and D13 with initial state $1s2s^22p^5(^3P)$ and lines D14 and D15 with initial state $1s2s^22p^5(^1P)$ (see (4)), relative to the intensity of the $KL_1L_{2,3}(^3P)$ diagram line, denoted as line A3 [14], as function of E_0. The relevant part of the K Auger spectrum, the energy region between 780 ... 800 eV, is shown in Fig. 2. The spectrum was taken with primary electron energy $E_0 = 40$ keV, for increasing the energy resolution to about $3 \cdot 10^{-4}$ the Auger electrons were decelerated by 600 V before they entered the spectrometer. The diagram line A3 and the satellite lines D11, 13, 14 and 15 are marked in Fig. 2. As can be seen there are many more overlapping lines in the region of satellite lines and only a line fitting procedure would give reasonable results.

For this fitting procedure the correct line shape has to be known. Close inspection of the line shapes, especially of the D satellites, shows strong asymmetries with a much broader high energy tail compared to the low energy side. This asymmetrical line shape is well known as one effect of the postcollision interaction (PCI). This has been found, together with an energy shift of the maximum of the line, in many experiments [25–27] and has been interpreted quantitatively only recently [28–30]. From the investigations [28–30] it follows that the postcollision interaction, the interaction between the scattered and the ionized electron with the Auger electron, never vanishes in the case of electron impact ionization even at very high incident energy E_0; there remains a small lineshift and a small distortion of the line shape due to the fact that the ionized electron has always a certain probability for being ejected with low velocity. In the case of the double ionization we expect a much larger PCI effect on the line shape and the line shift since now there are, in general, three electrons, the scattered and the two ionized electrons, which interact with the Auger satellite electron. In particular, it is the shake-off electron (we assume that the ionization in the $2p$ shell occurs mainly through the shake mechanism) which makes a large PCI contribution even at highest impact energies E_0. It has been predicted by theory [31] and verified by experiment [32] that the energy distribution of shake-off electrons goes approximately with

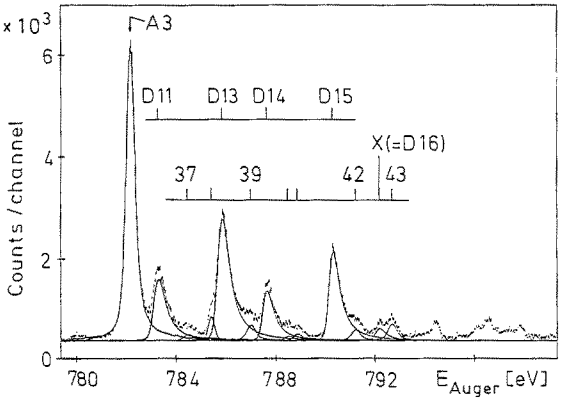

Fig. 2. Part of K Auger spectrum of neon with the diagram line A3 ($K-L_1L_{2,3}(^3P)$ transition) and $KL_{2,3}-LLL_{2,3}$ satellite lines D11, D13, D14 and D15. The spectrum was taken for primary electron energy $E_0 = 40$ keV and angle $\vartheta = 54.7°$ relative to the beam axis. The solid lines are the components obtained by a computer fit

$$W(E_s) \sim \exp(-E_s/E'(L)), \tag{10}$$

with E_s the energy of shake-off electron and $E'(L)$ the binding energy of an L electron in an atom ionized already in the K shell. It is this low energy distribution (10) which, in the sudden approximation, is independent of impact energy E_0 and therefore causes always a strong distortion of the line shape via PCI. From [30] we know that for $E_0 > 4E_B$, with E_B the binding energy of the inner-shell electron, the line shape of a diagram Auger line stays constant. Then it appears reasonable to assume the same also for the satellite line but with a much larger PCI distortion. The much larger PCI shift of $KL_{2,3}$ satellite lines of neon compared to that of the diagram lines has been measured recently [33].

The much larger line shape distortion of a D satellite line by PCI compared to the distortion of a diagram line has been found in the present investigation. In order to demonstrate this we have plotted in Fig. 3 that part of the spectrum of Fig. 2 which, after the diagram line A3 had been subtracted, contains mainly the satellite line D11. The solid line through the experimental values (heavy vertical bars in Fig. 3) is a theoretical PCI line

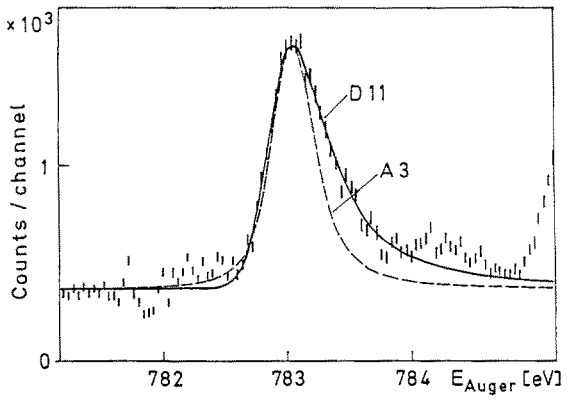

Fig. 3. Comparison of line shapes of the diagram line A3 with the $KL_{2,3}$ satellite line D11. The broader and asymmetric line shape of line D11 is due to the postcollision interaction

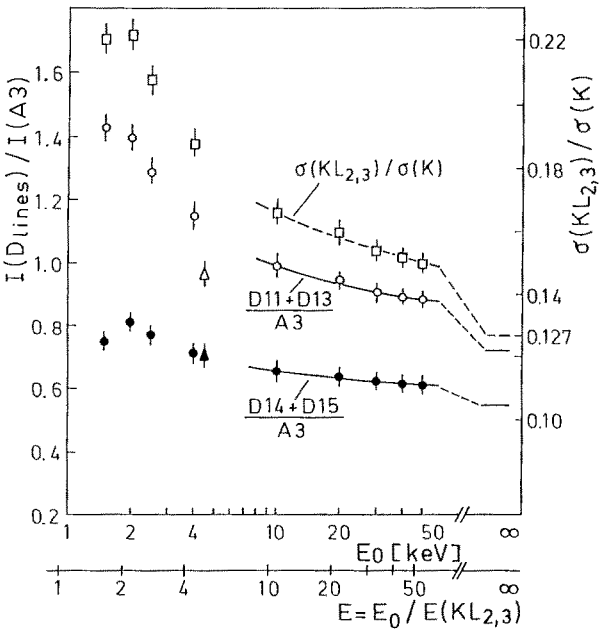

Fig. 4. Experimental intensity ratios $I(\mathrm{D11}+\mathrm{D13})/I(\mathrm{A3})$ and $I(\mathrm{D14}+\mathrm{D15})/I(\mathrm{A3})$ of $KL_{2,3}(^3P)$ and $KL_{2,3}(^1P)$ satellite lines relative to the diagram line A3 (left scale) for emission angle $\vartheta = 54.7°$ and as function of electron impact energy E_0 or of reduced energy $E_0/E(KL_{2,3})$. The experimental values found by Krause et al. [14] for $\vartheta = 90°$ are given by the symbols △ and ▲. Experimental ratio of cross sections $\sigma(KL_{2,3})/\sigma(K)$ (right scale) as function of energy E_0. The solid lines and the dashed line are computer fits to the experimental results according to (11). The asymptotic values of the ratios are indicated at the right side of the figure

calculated with the assumption that the PCI effect is solely due to the shake-off electron from the $2p$ shell, the small effect due to the ejected K shell electron has been neglected. As width $\Gamma(KL_{2,3}, {}^3P)$ of the initial state of satellite line D11 the theoretical value of 231 meV [34], increased by 8%, was taken. This increase of 8% takes into account that the experimental value $\Gamma(K) = 270$ meV [35, 36] is about 8% larger than the theoretical value of 255 meV [34]. The PCI line shape has been calculated using the Russek model [37] and assuming an energy distribution of the slow electron according to (10). Finally, the theoretical PCI line shape was convoluted with the Gaussian spectrometer function with width $\Delta E = 3 \cdot 10^{-4} \cdot E_{\mathrm{Auger}}$. Taking for $E'(L_{2,3})$ in (10) the value of 43.5 eV [14], the PCI line shape came out with a too small width. In order to reproduce the experimental line shape of line D11 (of Figs. 2 and 3) an unexpected small value of $E'(L_{2,3}) \cong 15$ eV had been taken. This can be explained, but only partly, by the fact that we have completely neglected the PCI effect of the ionized K shell electron. Also shown in Fig. 3 is the shape of the diagram line A3 (broken line). It can be clearly seen that the satellite line D11 is much broader and has a slower decrease of intensity at the high energy side than the diagram line. This difference in line shapes between the satellite and diagram lines has to be taken into account when the spectrum of Fig. 2 is decomposed into its components. In any case, this effect was not considered by Carlson et al. [1] because PCI after electron impact ionization became known only in 1976 [38].

The spectrum of Fig. 2 was decomposed into its components by using a fit program where for the diagram line A3 the line shape of the strongest diagram line A5 and for the satellite lines D11, D13, D14 and D15 theoretical PCI line shapes (with different level widths of initial states ^3P and ^1P [34]) were taken. For all other lines (except the lines 38 and X) a Lorentzian line shape with $\Gamma = 270$ meV which was convoluted by the spectrometer function was used. The different components of the spectrum are plotted in Fig. 2, their sum intensity (not shown is Fig. 2) fits the experimental spectrum very accurately between 780 and 794 eV. In order to get a good fit spectrum, the width of line 38 had to be taken somewhat smaller than 270 meV and for line X the shape of a D line had to be taken. Because of the latter fact we believe that line X is the satellite line D16 (see Sect. 4.3).

There is still another interesting feature of the spectrum of Fig. 2. Each of the satellite lines D11, D13, D14 and D15 is accompanied on its high energy side by a structure which could be an extra line but which could also be due to an angular momentum exchange in the postcollision interaction predicted by Niehaus and Zwakhals [39]. We postpone the discussion of this structure to Sect. 4.4. The intensities of these structures have not been included in the intensities of the corresponding satellite lines.

In Fig. 4 we have plotted the measured intensity ratios $I(\mathrm{D11}+\mathrm{D13})/I(\mathrm{A3})$ and $I(\mathrm{D14}+\mathrm{D15})/I(\mathrm{A3})$ as function of the incident energy E_0 and as function of the reduced incident energy $E = E_0/E(KL_{2,3})$. For comparison, also the values found by Krause et al. [14] are included in Fig. 4. It can be seen that both intensity ratios still decrease for reduced energies $E > 10$. In order to get the asymptotic ratio for $E \to \infty$ we fitted an expression

$$I(D\ \mathrm{lines})/I(\mathrm{A3}) = a + b(\ln E)^{-1} \qquad (11)$$

according to (1) to the experimental values in the energy region $E_0 = 10 \ldots 50$ keV (solid lines in Fig. 4). The

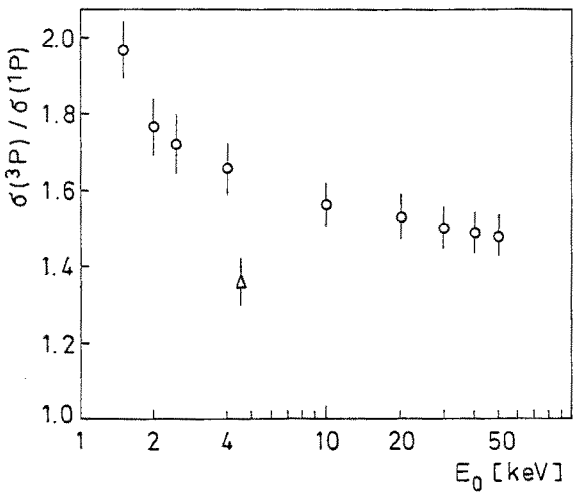

Fig. 5. Experimental ratio of cross sections $\sigma(KL_{2,3}\,^3P)/\sigma(KL_{2,3}\,^1P)$ for neon as function of primary electron energy E_0. O = present values, Δ = Krause et al. [14]

asymptotic values are about 20% smaller than those obtained by Krause et al. [14] for the energy of $E_0 = 4.5$ keV where the onset of constant ratio of $\sigma(KL_{2,3})/\sigma(K)$ was believed to occur [1].

The reason to have taken $E_0 = 10$ keV as lower limit of the energy region for the fit of expression (11) to the intensity ratios was because the ratio $I(\mathrm{D11}+\mathrm{D13})/I(\mathrm{D14}+\mathrm{D15})$ changes with energy E_0 and becomes practically constant only for $E_0 \geqq 10$ keV. This can be seen from the variation of the ratio $\sigma(^3P)/\sigma(^1P) = \sigma(KL_{2,3}\,^3P)/\sigma(KL_{2,3}\,^1P)$ with impact energy E_0 plotted in Fig. 5 and which is nearly equal to the ratio $I(\mathrm{D11}+\mathrm{D13})/I(\mathrm{D14}+\mathrm{D15})$. The variation of the ratio $\sigma(^3P)/\sigma(^1P)$ with energy E_0 has been deduced from the intensity ratios $I(\mathrm{D11}+\mathrm{D13})/I(\mathrm{A3})$ and $I(\mathrm{D11}+\mathrm{D13})/I(\mathrm{A3})$ of Fig. 4, the value of the ratio $\sigma(^3P)/\sigma(^1P)$ at $E_0 = 40$ keV was obtained by summing the intensities of all satellite lines with initial state $KL_{2,3}\,^3P$ and $KL_{2,3}\,^1P$ (see Table 1). The increase of cross section ratio $\sigma(^3P)/\sigma(^1P)$ for decreasing impact energy was not found earlier, rather a constant ratio was assumed [1]. On the other hand, the asymptotic value of the cross section ratio $\sigma(^3P)/\sigma(^1P)$ for large E_0 found in the present investigation to be 1.48(5) agrees rather well with the earlier value of 1.36 for $E_0 = 4.5$ keV [40, 14]. The reason for the deviation from the statistical value of 3 which is expected in the shake model and in the independent-particle picture was discussed by Chattarji et al. [41].

In Fig. 4 we have also plotted the ratio $\sigma(KL_{2,3})/\sigma(K)$ with its scale at the right side of the figure. This ratio follows from the intensity ratio $I(KL_{2,3} - LLL_{2,3})/I(KLL)$ of all $KL_{2,3} - LLL_{2,3}$ satellite lines to all KLL diagram lines at $E_0 = 40$ keV, the line intensities are given in Tables 1 and 2, and the variation of the intensity ratio $I(\mathrm{D11}+\mathrm{D13}+\mathrm{D14}+\mathrm{D15})/I(\mathrm{A3})$ from Fig. 4. By fitting an expression (11) to the experimental points (broken line in Fig. 4) the asymptotic value $a(KL_{2,3}/K) = 0.127(4)$ was obtained which is also indicated at the right side of Fig. 4. This value is 16% smaller than the value 0.152 found by Krause et al. for $E_0 = 4.5$ keV [14].

The asymptotic value of the experimental ratio $\sigma(KL_{2,3})/\sigma(K)$ cannot be compared directly with a theoretical value, which should be calculated in the shake-off model according to (2). Theoretically, only the total shake probability (shake-up (KL^*) and shake-off (KL)) has been calculated so far. The values obtained for

Table 1. Energies and intensities of D satellite lines of neon with initial configurations $1s\,2s^2\,2p^5$ and $1s\,2s\,2p^6$ and comparison with earlier results. The energies and intensities are relative to the diagram line A5 (Table 2) with energy 804.3 eV and intensity 100.0. The theoretical values [40] are normalized to the total intensity of D lines [14]

Line[a]	Initial state	Final state	Energy (eV)		Intensity		Theory [40]
			This exp. $E_0 = 40$ keV	[14] $E_0 = 4.5$ keV	This exp. $E_0 = 40$ keV	[14] $E_0 = 4.5$ keV	
D1	$1s\,2s^2\,2p^5(^3P)$	$2s^0\,2p^5(^2P)$	−73.55 (8)	−73.9 (2)	1.47 (10)	1.2 (1)	1.38
D3		$2s\;2p^4(^2P)$	−53.04 (8)	−53.3 (1)	1.18 (10)	1.1 (1)	1.30
D4		(^2S)	−50.48 (12)	−50.7 (2)	0.36 (10)	0.2 (1)	0.33
D7		(^2D)	−44.84 (12)	−45.0 (1)	1.92 (10)	1.8 (1)	1.67
D10		(^4P)	−36.18 (12)	−36.4 (2)	0.60 (10)	≈0.3	0.71
D11		$2s^2\,2p^3(^2P)$	−21.05 (8)	−21.2 (1)	3.18 (15)	3.2 (2)	3.15
D13		(^2D)	−18.46 (8)	−18.4 (1)	6.0 (2)	6.6 (2)	5.88
D2	$1s\,2s^2\,2p^5(^1P)$	$2s^0\,2p^5(^2P)$	−69.08 (8)	−69.2 (2)	1.15 (10)	0.9 (2)	1.09
D5		$2s\;2p^4(^2P)$	−48.67 (8)	−48.7 (1)	2.34 (10)	2.3 (1)	2.37
D6		(^2S)	–	−45.7 (3)	–	0.12 (5)	$2.4\cdot10^{-4}$
D9		(^2D)	(−40.4 (2))[c]	−40.5 (3)	–	≈0.1	$1.2\cdot10^{-3}$
D14		$2s^2\,2p^3(^2P)$	−16.67 (8)	−16.7 (2)	2.32 (15)	2.4 (3)	2.49
D15		(^2D)	−13.99 (8)	−13.9 (1)	4.10 (15)	4.8 (1)	4.65
D8[b]	$1s\,2s\,2p^6(^1S)$	$2s^0\,2p^5(^2P)$	−40.67 (12)	−40.5 (3) (D9)	0.26 (7)	≈0.1 (D9)	
D12[b]	$1s\,2s\,2p^6(^3S)$	$2s\,2p^4(^2D)$	−18.93 (16)	−19.0 (3) (X41)	0.54 (15)	0.2 (X41)	
D16	$1s\,2s\,2p^6(^1S)$	(^2D)	−12.13 (16)	−12.0 (3)	0.54 (15)	≈0.8	

[a] Line notation is taken from [14]. Final state of line D12 and initial state of line D16 differ from that given in [14] (see text)
[b] Lines labelled earlier [14] by D9 and X41 have now been identified as D8 and D12 (see text)
[c] Value obtained by subtracting the energy difference $E(\mathrm{D7}) - E(\mathrm{D1})$ from $E(\mathrm{D2})$

Table 2. Energies and relative intensities of KLL diagram lines of neon

Line	Transition	Energy (eV)		Rel. Intensity	
		Present	[14]	Present	[14]
A1	$KL_1L_1\,^1S$	748.14 (8)	748.1	10.1 (1)	9.95 (10)
A2	$KL_1L_{2,3}\,^1P$	771.71 (8)	771.6	28.3 (1)	28.2 (4)
A3	$KL_1L_{2,3}\,^3P$	782.24 (8)	782.1	10.3 (1)	10.2 (3)
A4	$KL_{2,3}L_{2,3}\,^1S$	800.60 (8)	800.6	15.6 (1)	15.6 (4)
A5	$KL_{2,3}L_{2,3}\,^1D$	804.30 (8)	804.3	100.0	100.0
A6	$KL_{2,3}L_{2,3}\,^3P_{0,2}$	–	807.4	–	0.07 (5)

$\sigma(KL+KL^*)/\sigma(K)$ by using DF wavefunctions are 0.216 [4] and 0.224 [5]. The corresponding experimental value is obtained by summing all intensities of satellite lines following KL shake-off and KL^* shake-up. The experimental value found by Krause et al. [14, 2] was $\sigma(KL+KL^*)/\sigma(K)=0.27(1)$, where about 63% is due to KL satellites. This experimental value is about 20% larger than the above theoretical values. If we reduce the KL satellite contribution to this ratio by 16%, according to the present result of the asymptotic value of $\sigma(KL_{2,3})/\sigma(K)$ compared to the earlier value [14], and leave the KL^* satellite contribution unchanged (this is justified by the results of Chap. 4.3 and Table 3), then the asymptotic value $\sigma(KL+KL^*)/\sigma(K)=0.24$ is obtained. This value is in better agreement with the theoretical results than the earlier value of 0.27.

4.2. *Alignment of double vacancy states* $1s2p\,^3P$ *and* ^1P

It was already pointed out that an alignment $\mathcal{A}_{20}\neq 0$ of the initial double vacancy states $1s2p\,^3P$ and ^1P cannot be expected within the shake-off model but could be possible if double collision processes are considered. Indeed, the increase of the cross section ratio $\sigma(KL_{2,3})/\sigma(K)$ for a decreasing impact energy below 4 keV found earlier was explained in part by multiple collisions [1]. Also, the unexpected change of cross section ratio of the multiplet states $\sigma(^3P)/\sigma(^1P)$ (Fig. 5) for E_0 below 4 keV might indicate that multiple collisions contribute and that a non-zero alignment and a non-isotropic angular distribution of Auger satellite electrons can be expected. Therefore, we have measured the intensity ratios $I(\mathrm{D11}+\mathrm{D13})/I(\mathrm{A3})$ and $I(\mathrm{D14}+\mathrm{D15})/I(\mathrm{A3})$ of Auger electrons for the two emission angles $\vartheta=54.7°$ and $\vartheta=90°$ (relative to the primary beam direction) and for the primary energies $E_0=1.5$, 2.0, 2.5 and 4.0 keV. The Auger spectra between $E_A=780\ldots796$ eV were measured with an energy resolution of the spectrometer of $5\cdot10^{-4}$, the spectra were decomposed into components with a fitting procedure as described in the previous section. Within an experimental error of $\pm2\%$ the intensity ratios are equal for both emission angles, i.e., the intensity of Auger D satellite lines is isotropic within our experimental errors. We therefore conclude that the alignment of the ^1P and ^3P states of the $KL_{2,3}$ vacancy configuration is zero with an upper limit of $|\mathcal{A}_{20}|<0.05(5)$.

4.3. *Relative intensities of K Auger lines*

In Sect. 4.1 we have seen that the shape of the Auger lines are distorted by the postcollision interaction. This effect decreases with increasing impact energy for the diagram Auger lines and for all other Auger lines where no shake-off transition is involved to create the initial state; but a small asymmetry remains even at infinite large impact energies [29, 30]. On the other hand, it was shown and discussed that the shake-off electron in the double ionization process KL makes *always* a large PCI contribution to the Auger line shape. In view of this and since the K Auger spectrum of neon [24, 1, 2] has served as critical test for the theory [42, 43], it is highly desirable to decompose once more the total K Auger spectrum of neon into its components by taking into account the different line shapes. In order to minimize the PCI effect on the shape of the diagram lines and of those lines, where no shake-off process is involved in the formation of the initial Auger state, we choose as impact energy $E_0=40$ keV.

In Fig. 6 the K Auger spectrum, measured at an emission angle $\vartheta=54.7°$, in the energy range 712–818 eV and with energy resolution $5\cdot10^{-4}$, is shown. The diagram lines (A lines), the $KL-LLL$ satellite lines (D lines) and the rest of lines have been indicated in the spectrum by tick bars. The energies and intensities of lines relative to the diagram line $KL_{2,3}L_{2,3}(^1D)$ (line A5) are given in Tables 1, 2 and 3. The energies of lines refer to the maxima of the lines, i.e. they include the PCI shift $\overline{\Delta\varepsilon}$. At an impact energy $E_0=40$ keV the PCI shift has the asymptotic value of $\overline{\Delta\varepsilon}=14$ meV [30] for the diagram lines (Table 2) and of $\overline{\Delta\varepsilon}=170$ meV for the D satellite lines (Table 1). The latter value follows from the PCI line calculation discussed in Sect. 4.1. On the other hand, the extra shift of the line maximum due to the convolution of an asymmetric PCI shape with a symmetric spectrometer function was corrected for those lines which have a PCI shape. For the D satellite lines this extra shift amounts to 70 meV, for the diagram lines this extra shift is too small and can be neglected.

We have also listed in Tables 1 and 2 the energies and intensities of K Auger lines found by Krause et al. [14] for an impact energy $E_0=4.5$ keV and an emission angle $\vartheta=90°$. For a comparison between the present values and the earlier values [14] of Table 1 one should bear in mind that according to Fig. 4 the relative intensities of the D lines decrease between $E_0=4.5$ keV and

Table 3. Relative energies and intensities of K Auger lines, except A lines and D lines. The energies and intensities are relative to the diagram line A5 (Table 2) with $E_A = 804.30$ eV and intensity 100.0. In the last column the line designation by Krause et al. [14] is given

Line No	Energy[a]	Intensity	Designation [14]
1	−78.00 (8)	0.37 (3)	X9
2	−76.76	0.02 (1)	–
3	−75.42	0.08 (3)	X10
4	−74.38	0.05 (2)	–
5	−72.66	0.07 (3)	X11
6	−72.10	0.24 (4)	X12
7	−70.61	0.11 (3)	X13
8	−68.17	0.17 (4)	X14
9	−67.09	0.19 (4)	X15
10	−66.05	0.24 (3)	X16
11	−64.17	0.03 (2)	X17
12	−62.52	0.17 (2)	X19
13	−59.10	0.30 (3)	X22
14	−57.60	0.11 (4)	X23
15	−55.19	0.19 (8)	X24
16	−54.35	0.14 (4)	X25
17	−51.28	0.35 (3)	X26
18	−49.45	0.15 (5)	–
19	−47.75	0.14 (6)	X27
20	−47.27	0.30 (5)	–
21	−43.76	1.25 (8)	X28
22	−42.39	0.07 (4)	X29
23	−40.26	0.56 (5)	X31
24	−39.74	0.12 (7)	–
25	−39.00	0.70 (7)	X32
26	−37.34	0.09 (5)	X33
27	−36.94	0.11 (5)	X34
28	−35.04	0.19 (7)	X35
29	−34.70	0.27 (7)	–
30	−31.48	0.19 (9)	–
31	−31.11	0.09 (6)	–
32	−30.62	0.06 (4)	–
33	−27.27	0.13 (3)	X38
34	−26.35	0.05 (3)	–
35	−25.79	0.17 (3)	X39
36	−24.78	0.12 (3)	X40
37	−19.85	0.28 (10)	–
38	−17.33	0.54 (20)	–
39	−15.78	0.12 (8)	X43
40	−15.42	0.30 (15)	X43
41	−13.10	0.44 (8)	X44
42	−11.62	0.72 (15)	X45
43	− 9.91 (8)	0.79 (8)	$C\alpha 2$
44	− 8.82	0.20 (8)	$C\alpha 3$
45	− 8.26	0.36 (10)	$C\alpha 4$
46	− 7.78	0.77 (10)	$C\alpha 5$
47	− 7.14	0.30 (10)	$C\alpha 6$
48	− 6.54	0.44 (8)	$C\alpha 7$
49	− 4.41	0.96 (40)	$C\alpha 9$
50	+ 1.76	0.60 (30)	–
51	+ 3.16	0.20 (8)	$B\alpha 2$
52	+ 6.89	0.48 (5)	$B\alpha 5$
53	+ 8.78	0.05 (3)	$B\alpha 6$

[a] Error of energy ±0.15 eV if not otherwise stated

$E_0 = 40$ keV. In Table 1 also theoretical intensities [40] normalized to the experimental total $KL_{2,3} - LLL_{2,3}$ intensity [14] are given.

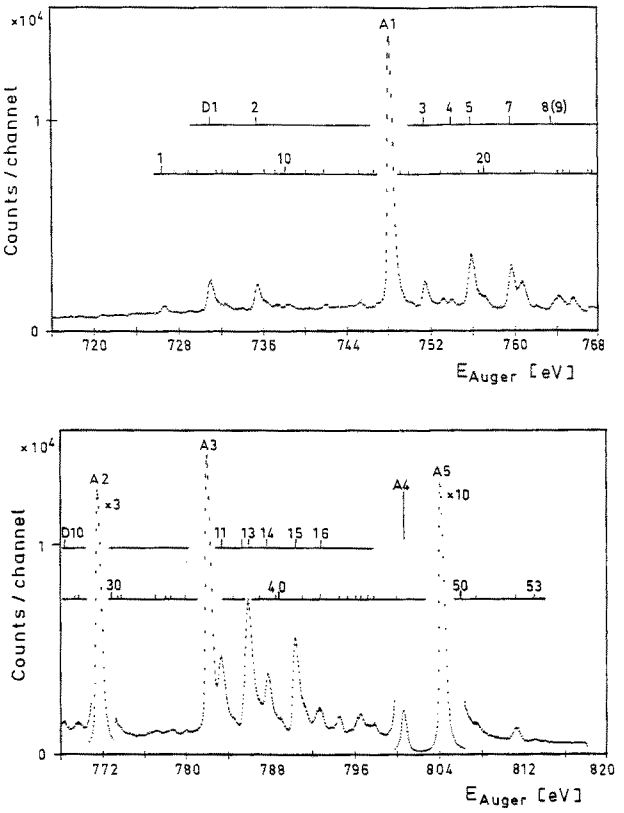

Fig. 6. K Auger spectrum of neon taken for primary electron energy $E_0 = 40$ keV and emission angle $\vartheta = 54.7°$ relative to the beam axis. The energies and intensities of diagram lines (A lines), of $KL-LLL$ satellite lines (D lines) and all other lines are given in Tables 2, 1 and 3, respectively

The assignment of a few lines of Table 1 had to be changed compared to that given earlier [14]. The reason for this reassignment is that now the energies of initial states $KL_1\,^1S$ and ^3S are accurately known from the X-ray emission spectrum of KL states of neon [44]. With the energies of the final LL states [45], the KL_1 energies are obtained to be $E(KL_1\,^1S) = 949.81$ eV and $E(KL_1\,^3S) = 943.03$ eV. From the calculation of $KL_1 - LLL_1$ transition probabilities [40] follows that almost all intensity is contained in only three lines, two lines (D8 and D16) with initial state $KL_1\,^1S$ and one line (D12) with initial state $KL_1\,^3S$. The correct final states are given in Table 1, where the final state of line D12 differs from that given in [14]. Using the initial state energies of $KL_1\,^1S$ and ^3S and of $KL_{2,3}\,^1P$ and ^3P ($E(KL_{2,3}\,^1P) = 921.37$ eV and $E(KL_{2,3}\,^3P) = 916.95$ eV [44]) and the relevant transition energies $KL_{2,3} - LLL_{2,3}$ of Table 1 one obtains for the energies of lines D8, D12 and D16 the following values: $E(\mathrm{D8}) = -40.67(8)$ eV, $E(\mathrm{D12}) = -18.76(12)$ eV, $E(\mathrm{D16}) = -11.98(12)$ eV. These values agree well with the experimental energies of lines found in the present investigation, the lines are therefore identified as D8, D12 and D16. Further support for this identification is given by the expected theoretical relative intensities [40] which are $I(\mathrm{D8}):I(\mathrm{D12}):I(\mathrm{D16}) = 1:1.7:1.7R$, where R is the cross section ratio $\sigma(KL_1\,^3S)/\sigma(KL_1\,^1S)$. Statistically one expects $R = 3$, but a value closer to one is suggested if the result of Fig. 5

is taken into account. The experimental relative intensities of relevant lines are $I(D8)=0.26(7)$, $I(D12)=0.54(15)$, and $I(D16)=0.54(15)$ and agree reasonably well with the theoretical values.

Furthermore, we believe that the intensity of line D9 is too small (see theoretical value in last column of Table 1) to be detected at all. The energy of this line can be calculated by $E(D9)=E(D2)-(E(D7)-E(D1))$ and yields the value $-40.4(2)$ eV (given in parenthesis in Table 1). This value is very close to the energy of line D8, we therefore believe that the line labelled earlier as line D9 [14] is actually line D8, this has been indicated in Table 1. In order to get agreement with the present identification the line labelled earlier [14] as D12 has to be discarded for energy reasons and the earlier line X41 has to be taken instead.

The energies and relative intensities of KLL diagram lines (A lines) of the present investigation (Table 2) agree very well with the results of Krause et al. [14]. The relative intensities and energies of the other lines (Table 3) agree in general with the earlier values [14] with a few exemptions for the intensities. Also a few lines of Table 3 have no corresponding lines in the earlier investigation and vice versa; in each of these cases the line intensity is very small.

4.4. Angular momentum exchange in postcollision interaction

Niehaus and Zwakhals [39] have predicted that angular momentum exchange in the postcollision interaction should lead to observable structures in the intensity distribution of an Auger line. These structures should occur at energies

$$\varepsilon_* = \varepsilon_0 + \{2[l_f(l_f+1) - l_i(l_i+1)]\}^{-1} \tag{12}$$

with ε_0 the nominal Auger energy and l_i and l_f the initial and final orbital angular momenta of the slow electron (atomic units are used in (12)). In order that an angular momentum exchange is best observable it must be ensured that the slow electron is in a state with definite orbital angular momentum l_i. This is the case either for a photoelectron or for the shake-off electron but not for the electron ionized by electron impact. For example, the $2p$ electron of neon is ejected as p electron by the shake-off process. Therefore, the PCI line shape of an Auger satellite line following shake-off is distinguished to investigate this effect of angular momentum exchange in the postcollision interaction. In the present case the shake-off electron has $l_i=1$. If one, two or three units of angular momentum are exchanged then $l_f=2,3$ and 4 and the energy difference $(\varepsilon_*-\varepsilon_0)$ according to (12) is 3.4, 1.36 and 0.76 eV, respectively. The Auger electron of a $KL_{2,3}-LLL_{2,3}$ transition is ejected with $l'=0,1$ or 2 (see Table 4), but even an s Auger electron can exchange angular momentum with the slow shake-off electron.

We have searched for these structures due to angular momentum exchange in the postcollision interaction. An evaluation of the relative energies $\varepsilon_*-\varepsilon_0$ of lines of Table 3 in relation to the more intense D lines of Table 1 yields lines (see Table 4) which are rather close to the expected values of 1.36 and 0.76 eV. Although an interpretation of these lines in terms of angular momentum exchange is rather tempting the following facts are against such an interpretation.

Table 4. Energies ε_* of lines on the high-energy side of a satellite line relative to the position ε_0 of satellite line. The orbital angular momentum l' of ejected Auger electron is given in column 2, the line numbers in parenthesis in the last column refer to those of Table 3

Line	l'	$\varepsilon_*-\varepsilon_0$ [eV]
D1	0	0.89 (line 5), 1.45 (line 6), 2.94 (line 7)
D2	0	0.91 (line 8), 1.99 (line 9)
D3	1	1.76 (line 17)
D5	1	0.92 (line 19), 1.40 (line 20)
D7	1	1.08 (line 21), 2.45 (line 22)
D11	0,2	1.20 (line 37), 2.12 (line 38)
D13	2	1.13 (line 39)
D14	0,2	0.89 (line 40), 1.25 (line 41)
D15	2	0.89 (line 42), 1.86 (line D16)

According to Niehaus and Zwakhals [39] the visibility of the momentum exchange structure increases for decreasing energy of the slow electron. A reinvestigation of the Auger line shape of the $N_5-O_{2,3}O_{2,3}(^1S_0)$ transition distorted by PCI following near threshold photoionization of the $4d_{5/2}$ electron of xenon [46] (here we have again $l_i=1$ and $l'=2$) did not find any clear structure even not for the very small energy of the photoelectron of 0.5 eV [47]. On the other side, if the lines of Table 4 were due to angular momentum exchange, then one could expect in the case of PCI with 0.5 eV photoelectrons a structure on the high-energy side of the $N_5-O_{2,3}O_{2,3}(^1S_0)$ Auger line (with $\varepsilon_*-\varepsilon_0\approx 0.76$ eV) with roughly 10% relative intensity. The negative experimental result indicates that the probability for the necessary angular momentum exchange of $\Delta l=l_f-l_i=3$ is apparently very small. Indeed, the upper bound of angular momentum exchange Δl between two interacting electrons has been estimated to be $\Delta l \leqq 1/v_f$ where v_f is the velocity in atomic units of the faster electron [48, 49]. With the energy of the $N_5-O_{2,3}O_{2,3}(^1S_0)$ Auger electron of 30 eV the upper bound is $\Delta l \leqq 0.7$, therefore an exchange of $\Delta l=3$ is rather unlikely.

We now turn back to the $KL_{2,3}$ Auger satellite electrons of neon. Taking as mean energy of these electrons a value of 750 eV then the upper bound for an angular momentum exchange is $\Delta l \leqq 1/7.4$ and thus much smaller than in the case of $N_5-O_{2,3}O_{2,3}(^1S_0)$ Auger electrons of xenon. We therefore conclude that the lines of Table 4 cannot be interpreted as structures caused by angular momentum exchange, we rather assign these lines to Auger lines with very small intensity.

We thank B. Kämmerling, W. Sandner, V. Schmidt and M. Völkel for helpful discussions. Part of this work has been supported by the Deutsche Forschungsgemeinschaft.

References

1. Carlson, T.A., Moddeman, W.E., Krause, M.O.: Phys. Rev. A **1**, 1406 (1970)
2. Krause, M.O.: J. Phys. (Paris) **32**, C4-67 (1971)
3. Krause, M.O.: Proceedings of the International Conference on Inner-Shell Ionization Phenomena and Future Applications, Atlanta 1972, Fink, R.W., Manson, S.T., Palms, J.M., Rao, P.V. (eds.), Report No Conf-720404, p. 1586ff. Oak Ridge: USEAK Technical Information Center 1973
4. Carlson, T.A., Nestor Jr., C.N.: Phys. Rev. A **8**, 1887 (1973)
5. Löw, W., Genz, H., Richter, A., Dyall, K.G.: Phys. Lett. **100** A, 130 (1984)
6. Åberg, T.: Ann. Acad. Sci. Fenn. A VI **308**, 1 (1969)
7. Åberg, T.: Proceedings of the International Conference on Inner-Shell Ionization Phenomena and Future Applications, Atlanta 1972, Fink, R.W., Manson, S.T., Palms, J.M., Rao, P.V. (eds.), Report No Conf-720404, p. 1506ff. Oak Ridge: USEAC Technical Information Center 1973
8. Chattarji, D., Mehlhorn, W., Schmidt, V.: J. Electron. Spectrosc. Relat. Phenom. **13**, 97 (1978)
9. Jamison, K.A., Richard, P.: Phys. Rev. Lett. **38**, 484 (1977); Phys. Rev. A **17**, 1642 (1978)
10. Cleff, B.: Acta Phys. Pol. A **61**, 285 (1982)
11. Ricz, S., Kádár, I., Shchegolev, V.A., Varga, D., Végh, J., Berenji, D., Hock, G., Sulik, B.: J. Phys. B **19**, L411 (1986)
12. Kocbach, L., Taulbjerg, K.: Xth International Conference on the Physics of Electronic and Atomic Collisions, Paris 1977, Abstracts, p. 44
13. Merzbacher, E., Wu, J.: Xth International Conference on the Physics of Electronic and Atomic Collisions, Paris 1977, Abstracts, p. 46
14. Krause, M.O., Carlson, T.A., Moddeman, W.E.: J. Phys. (Paris) **32**, C4-139 (1971)
15. Mehlhorn, W.: Phys. Lett. **26** A, 166 (1968)
16. Cleff, B., Mehlhorn, W.: J. Phys. B **7**, 593 (1974)
17. Berezhko, E.G., Kabachnik, N.M.: J. Phys. B **10**, 2467 (1977)
18. Kabachnik, N.M., Lee, I.S., Lee, O.V.: High-energy ion-atom collisions. In: Berenyi, D., Hock, G. (eds.) Lecture Notes in Physics, Vol. 294, p. 220. Berlin, Heidelberg, New York: Springer 1988
19. Kabachnik, N.M., Sazhina, I.P.: J. Phys. B **17**, 1335 (1984)
20. Mehlhorn, W.: Electron spectroscopy of Auger and autoionizing states: experiment and theory. Lecture Notes, University of Aarhus, 1978, p. 124 (unpublished)
21. Wigger, J., Altevogt, H., Brüssermann, M., Richter, G., Cleff, B.: J. Phys. B **17**, 4721 (1984)
22. Mehlhorn, W., Breuckmann, B., Hausmann, D.: Phys. Scr. **16**, 177 (1977)
23. Weber, W., Breuckmann, B., Huster, R., Menzel, W., Mehlhorn, W., Chen, M.H., Dyall, K.G.: J. Electron. Spectrosc. Relat. Phenom. **47**, 105 (1988)
24. Körber, H., Mehlhorn, W.: Z. Phys. **191**, 217 (1966)
25. Huster, R., Mehlhorn, W.: Z. Phys. A – Atoms and Nuclei **307**, 67 (1982)
26. Helenelund, K., Hedman, S., Asplund, L., Gelius, G., Siegbahn, K.: Phys. Scr. **27**, 245 (1983)
27. Gräf, D., Hink, W.: J. Phys. B **20**, 2677 (1987)
28. Sandner, W.: J. Phys. B **19**, L863 (1986)
29. Sandner, W.: In: Electronic and atomic collisions. Invited papers of the XVth Conference on the Physics of Electronic and Atomic Collisions, Brighton, 1987, Gilbody, H.B., Newell, W.R., Read, F.H., Smith, A.C.H. (eds.), p. 177. Amsterdam: North-Holland 1988
30. Sandner, W., Völkel, M.: Phys. Rev. Lett. **62**, 885 (1989)
31. Levinger, J.S.: Phys. Rev. **90**, 11 (1953)
32. Krause, M.O., Carlson, T.A., Dismukes, R.D.: Phys. Rev. **170**, 37 (1968)
33. Starke, K., Gräf, D., Hink, W.: J. Phys. B **21**, 4217 (1988)
34. Chen, M.H., Crasemann, B.: Phys. Rev. A **12**, 959 (1975)
35. Svensson, S.N., Mårtensson, N., Basilier, E., Malmquist, P.A., Gelius, U., Siegbahn, K.: Phys. Scr. **14**, 141 (1976)
36. Krause, M.O., Oliver, J.H.: J. Phys. Chem. Ref. Data **8**, 329 (1979)
37. Russek, A., Mehlhorn, W.: J. Phys. B **19**, 911 (1986)
38. Ohtani, S., Nishimura, H., Suzuki, H., Wakya, K.: Phys. Rev. Lett. **36**, 863 (1976)
39. Niehaus, A., Zwakhals, C.J.: J. Phys. B **16**, L135 (1983)
40. Schmidt, V.: Proceedings of the International Conference on Inner-Shell Ionization Phenomena and Future Applications, Atlanta 1972, Fink, R.W., Manson, S.T., Palms, J.M., Rao, P.V. (eds.), Report No Conf-720404, p. 548ff. Oak Ridge: USEAC Technical Information Center 1973
41. Chattarji, D., Mehlhorn, W., Schmidt, V.: J. Electron. Spectrosc. Relat. Phenom. **13**, 97 (1978)
42. Asaad, W.N.: Nucl. Phys. **66**, 494 (1965)
43. Kelly, H.P.: Phys. Rev. A **11**, 556 (1975)
44. Ågren, H., Nordgren, L., Selander, L., Nordling, C., Siegbahn, K.: J. Electron. Spectrosc. Relat. Phenom. **14**, 27 (1978)
45. Moore, Ch.E.: Atomic energy tables. Vol. I. Natl. Bur. Stand., Circular 467 (1971)
46. Borst, M., Schmidt, V.: Phys. Rev. A **33**, 4456 (1986)
47. Kämmerling, B., Schmidt, V.: Private communication
48. Fano, U.: J. Phys. B **7**, L401 (1974)
49. Heideman, H.G.M., van Ittersum, T., Niehus, G., Hol. V.M.: J. Phys. B **8**, L26 (1975)